



Chaotic fluctuations in Greenland outlet glaciers limit predictability of a future ice sheet collapse

Kolja Kypke^{1,2}, Marisa Montoya^{3,4}, Alexander Robinson⁵, Jorge Alvarez-Solas^{3,4}, Jan Swierczek-Jereczek^{3,4}, and Peter Ditlevsen¹

¹Physics of Ice, Climate and Earth, Niels Bohr Institute, University of Copenhagen, Copenhagen, Denmark

²Department of Mathematics and Statistics, University of Guelph, Guelph, Canada

³Department of Earth Physics and Astrophysics, Complutense University of Madrid, Madrid, Spain

⁴Geosciences Institute, CSIC-UCM, Madrid, Spain

⁵Alfred Wegener Institute, Helmholtz Centre for Polar and Marine Research, Potsdam, Germany

Correspondence: Kolja Kypke (kkypke@uoguelph.ca)

Abstract. The future evolution of the Greenland ice sheet (GrIS) depends on the intensity and the speed of climate change. By applying different rates of temperature change in a state-of-the-art comprehensive ice-sheet model coupled to a regional energy-moisture balance atmospheric model, oscillations in the total ice-sheet volume are found under warming magnitudes between 1.0 and 1.3 K above present-day temperatures. These are located in the northwestern drainage basin of the GrIS and are due to two ice streams which alternate between fast and slow basal velocities, manifesting in a build-up/surge variability. These ice streams interact due to their spatial proximity, resulting in irregular periodicity. The ice streams appear in a region where tipping of the entire GrIS begins, leading the oscillations to affect the tipping behaviour. These oscillations directly impact the time it takes before the ice sheet collapses at a given external forcing magnitude by hundreds of thousands of years for an ensemble of rates of forcing and initial conditions. These long tipping times are proposed to be due to chaotic transients. Our results suggest that ice-stream oscillations are a potential source of internal chaotic variability in ice sheets that affect tipping behaviour, thereby complicating prospects of anticipating such a tipping.

1 Introduction

The Greenland ice sheet (GrIS) is one of the principal tipping elements in Earth's climate system (Armstrong McKay et al., 2022), meaning it could experience a massive and potentially irreversible change when an external forcing parameter, specifically the global mean temperature, increases beyond a critical threshold known as a 'tipping point' (Robinson et al., 2012). This phenomenon is also termed 'bifurcation-induced tipping' (b-tipping). This tipping involves the large-scale loss of ice mass (or 'collapse' of the ice sheet) through melting and has a straightforward impact on the rest of the Earth by raising the global sea level (Gregory et al., 2004; Rignot et al., 2011).

Tipping of the GrIS can occur due to the presence of two strong positive feedbacks: First, a decrease in ice-sheet thickness means that the temperature of the ice surface increases, promoting further melting, known as the melt-elevation feedback. The second is the decrease of the surface albedo as a result of the retreat of the ice sheet increasing the amount of solar



energy absorbed, known as the ice-albedo feedback. In steady state, where the ice sheet is in mass balance, the dynamics must, however, be dominated by negative feedbacks: As atmospheric temperatures increase, so does the precipitation and the surface mass balance, leading to a thickening of the ice sheet. Furthermore, the melt-elevation feedback is reduced by the effect of glacial isostatic adjustment: when ice thins, the resulting bedrock uplift partially compensates the reduced surface elevation and thus the surface melt. This effect is, however, mainly relevant on long time scales (Wake et al., 2016; Zeitz et al., 2022). The atmospheric temperature is considered the critical parameter. As it increases, the negative feedbacks weaken and at the bifurcation point, the negative feedback no longer control the state and the positive feedbacks will force it into the alternative state.

While the critical temperature for tipping of the GrIS has been assessed in different studies (Gutiérrez-González et al.; Höning et al., 2023; Robinson et al., 2012; Zeitz et al., 2022), the effect of the rate of change of the forcing on the tipping behaviour has not yet been investigated. The feedbacks that determine the stability of the GrIS are influenced strongly by the surface air temperature of Greenland, which is increasing at a rapid pace (Intergovernmental Panel On Climate Change (IPCC), 2023). In non-autonomous systems with multiple dynamic time scales, high rates of forcing compared to the time scale for restoring to the equilibrium state could lead to a tipping of the system at a forcing less than the bifurcation point, a phenomenon known as ‘rate-induced tipping’ (r-tipping) (Ashwin et al., 2012; Feudel, 2023).

The bulk of the GrIS evolves over time according to slow shear flow, but areas of fast flowing ice, such as topographically confined outlet glaciers or large ice streams, represent a source of variability with a faster dynamic timescale. Ice streams in particular are relevant, as they are characterized by sliding of ice at the base due to a till that is saturated with water. A fast warming rate can lead to an easier saturation of the base because it cannot be compensated by the drainage rate, activating ice streams and increasing mass loss. The discharge of ice through ice streams contributes a large amount to the total ice-sheet mass loss despite their relatively small spatial extent (The IMBIE Team, 2020; Van Den Broeke et al., 2009). Furthermore, ice streams have accelerated due to increased atmospheric and oceanic forcing, contributing up to 50% of the GrIS mass loss in the last decades (Holland et al., 2008; Howat et al., 2008; Khan et al., 2014; Krabill et al., 2004; Larocca et al., 2023; Luthcke et al., 2006; Rignot and Kanagaratnam, 2006; Rignot et al., 2011; Trusel et al., 2018).

Rate-induced tipping of a component of the Earth system has been investigated previously in comprehensive models of the Atlantic Meridional Overturning Circulation (AMOC) (Lohmann and Ditlevsen, 2021) and the west Antarctic ice sheet (Swierczek-Jereczek et al., 2025). The rate of forcing is also important when considering the ability to prevent a transition after overshooting a tipping point by imposing a subsequent cooling (Bochow et al., 2023). In this study, we use a state-of-the-art ice-sheet model coupled to a regional atmospheric energy-moisture balance model to investigate the GrIS response under different magnitudes and rates of warming in order to determine whether r-tipping of the GrIS is possible.



2 Methods

2.1 Model description

The model used in this study is the three-dimensional thermomechanical ice-sheet model Yelmo (Robinson et al., 2020) coupled with the regional energy-moisture balance climate model REMBO (Robinson et al., 2010). This model setup is similar to that of Robinson et al. (2012) but with a newer ice-sheet model. The model domain covers the entirety of Greenland at a horizontal resolution of 16 km. The surface mass balance (SMB) is determined by the temperature and precipitation calculated by REMBO. The SMB can be separated into a positive contribution from the precipitation and a negative contribution resulting from surface melt. The latter is calculated using an insolation-temperature melt method (ITM), whereby insolation and albedo are explicitly taken into account. The isostatic adjustment of the bedrock under the ice sheet uses the elastic lithosphere-relaxing asthenosphere (ELRA) model (Meur and Huybrechts, 1996) with a relaxation timescale of 3000 years.

To compute the ice dynamics, Yelmo uses the depth-integrated viscosity approximation (Goldberg, 2011; Robinson et al., 2022). The basal frictional stress $\tau_b = (\tau_{b,x}, \tau_{b,y})$ is modelled using a regularized Coulomb friction law (Schoof, 2005; Joughin et al., 2019),

$$\tau_b = -c_b \left(\frac{|\mathbf{u}_b|}{|\mathbf{u}_b| + u_0} \right)^q \frac{\mathbf{u}_b}{|\mathbf{u}_b|}, \quad (1)$$

where $\mathbf{u}_b = (u_b, v_b)$ is the basal velocity vector, $u_0 = 100 \text{ m a}^{-1}$ and $q = 0.2$ are empirical parameters derived from laboratory experiments (Zoet and Iverson, 2020), and c_b is a field defining the bed-friction coefficient. The threshold speed u_0 allows the basal stress to saturate at large velocities, where it becomes independent of basal velocity (Blasco et al., 2024; Zoet and Iverson, 2020). The coefficient c_b depends linearly on the effective pressure N at the base of the ice,

$$c_b = \lambda N. \quad (2)$$

The factor λ represents the till strength of the bedrock and depends on the elevation above or below sea level. This factor leads to increased sliding velocity by reducing basal friction at lower elevations, owing to the till in these areas being composed primarily of sediments that are softer and more easily deformable. A similar elevation-dependent till strength is also seen in Albrecht et al. (2020) and Martin et al. (2011).

The effective pressure \hat{N} differs from the overburden pressure depending on the basal water content, following the parameterization of Bueler and van Pelt (2015):

$$\hat{N} = N_0 \left(\frac{\delta P_0}{N_0} \right)^s 10^{\frac{c_0}{c_c} (1-s)}. \quad (3)$$

The effective pressure decreases with increasing till saturation $s = H_w / H_{w,\max}$ to a minimum value of δP_0 at $s = 1$. The parameter P_0 is the overburden pressure, with $\delta = 0.02$ being an empirical minimum fraction. This means that the effective pressure at the base is equal to 2% of the overburden pressure when the till is saturated, and any excess water is considered to be drained from the system (Bueler and van Pelt, 2015). The parameter $N_0 = 1000 \text{ Pa}$ is a reference pressure at a reference



void ratio $e_0 = 0.69$, and $C_c = 0.12$ is the coefficient of compressibility of the till. Finally, since the overburden pressure is an upper limit for the effective pressure, the minimum of the two is taken,

$$N = \min \left\{ P_0, \hat{N} \right\}. \quad (4)$$

85 The basal water layer thickness H_w changes with the basal mass balance \dot{b}_g and is removed via a constant drainage rate C_d ,

$$\frac{\partial H_w}{\partial t} = -\frac{\rho_i}{\rho_w} \dot{b}_g - C_d, \quad (5)$$

where ρ_i and ρ_w are the ice and water densities, respectively, and \dot{b}_g is the basal mass balance,

$$\dot{b}_g = -\frac{1}{\rho_i L} \left(Q_b + k \frac{\partial T}{\partial z} \Big|_b + Q_r \right). \quad (6)$$

The function \dot{b}_g therefore converts the heat flux at the base to a melt rate via the latent heat of ice fusion, L . The heat flux
90 consists of the heat generated by friction due to sliding of the ice along the base Q_b as well as the heat conducted into the column of ice above given by the coefficient of conduction of ice k and the temperature gradient of the ice at the base $\frac{\partial T}{\partial z} \Big|_b$. In addition to this, there is a geothermal heat flux boundary condition Q_{geo} imposed 2 km below the surface and the heat diffuses vertically through the bedrock. The term Q_r is then the flow of heat into the ice at the interface of bedrock and ice.

2.2 Experimental setup and boundary conditions

95 The model is first run to equilibrium for 400 ka to arrive at an initial state (Fig. 1) corresponding to the present-day GrIS. The ice-sheet thickness and bedrock topography are initialized using data from version 5 of the BedMachine mapping of Greenland (Morlighem et al., 2017). The surface boundary conditions of Yelmo are determined by REMBO, which uses the ERA-40 climatology (Uppala et al., 2005) as its boundary conditions. The states of the GrIS at 200 ka and 300 ka are also saved as initial states, representing a small perturbation to the initial state at 400 ka. This is the starting point from which the model is
100 forced in subsequent simulations. The use of an ensemble of multiple initial states is not common for ice-sheet simulations, but is implemented to test the robustness of the results and a possible dependence on initial conditions.

By definition, r-tipping occurs at a forcing temperature below the critical b-tipping value, so the latter must first be estimated. To estimate the bifurcation point of the GrIS, the sea-level summer air temperature and ocean temperature at the boundaries of REMBO are gradually increased, as in Robinson et al. (2012). This regional summer temperature anomaly is approximately
105 equivalent to a global mean temperature increase. This forcing is applied using an adaptive quasi-equilibrium forcing (AQEF) function starting at each of the three initial states. This AQEF interactively adapts the forcing in order to maintain the ice sheet in a quasi-steady state by ensuring that the rate of ice-volume loss stays below a given threshold, equal to 2 gigatons per year averaged over 100 years. The forcing increase is done in an adaptive way such that the longer it takes the model to equilibrate, the less the forcing is subsequently increased. In this way, the forcing parameter does not increase while the tipping
110 is occurring.

Once the tipping point has been estimated, it is used to determine a range of parameters for the subsequent ramping experiments that are used to assess the possibility of r-tipping. In these ramping experiments, the forcing is increased at a linear rate

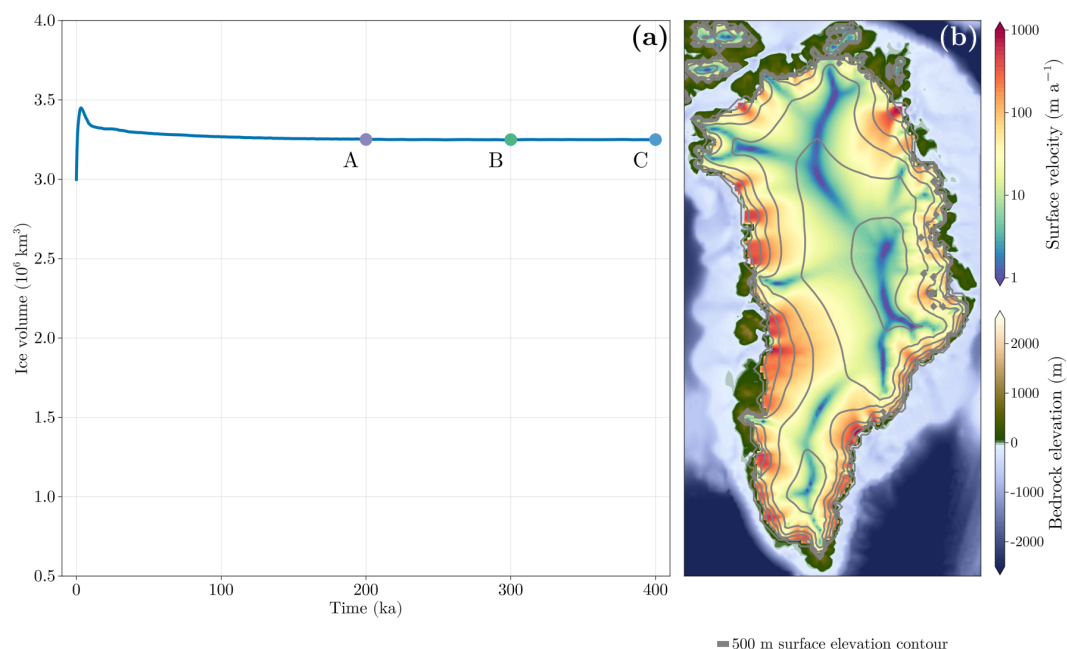


Figure 1. (a): Ice volume time series of the equilibrium simulation for the three initial states A to C. (b): Ice sheet extent of the initial state C at the end of the 400 ka spin-up run.

to some value less than the tipping point. Thereafter, the forcing is kept constant and the ice sheet is allowed to equilibrate over 400 ka. An ensemble of simulations is generated by applying different rates of increase and maximal forcing values, allowing the effect of the rate and magnitude of warming to be evaluated. These ramping experiments are also performed starting at each of the three initial states to investigate the effect of different initial conditions.

3 Results

3.1 Tipping of the ice sheet

Figure 2 shows the ice volume as a function of the forcing parameter, the regional summer temperature anomaly, for the three initial states. There is clear tipping behaviour for a forcing of +1.275 K, which is essentially independent of the choice of initial state. This tipping resembles what is expected for a saddle-node bifurcation.

The retreat of the GrIS during the tipping event is seen in Fig. 3. Spatially, the retreat begins in the north. Due to the similarities in the model setups between this study and that of Robinson et al. (2012), the spatial tipping pattern is equivalent. The pattern of ice sheet loss is also similar to that of Zeitz et al. (2022) (their Fig. 3a) albeit without the regrowth of the ice sheet.

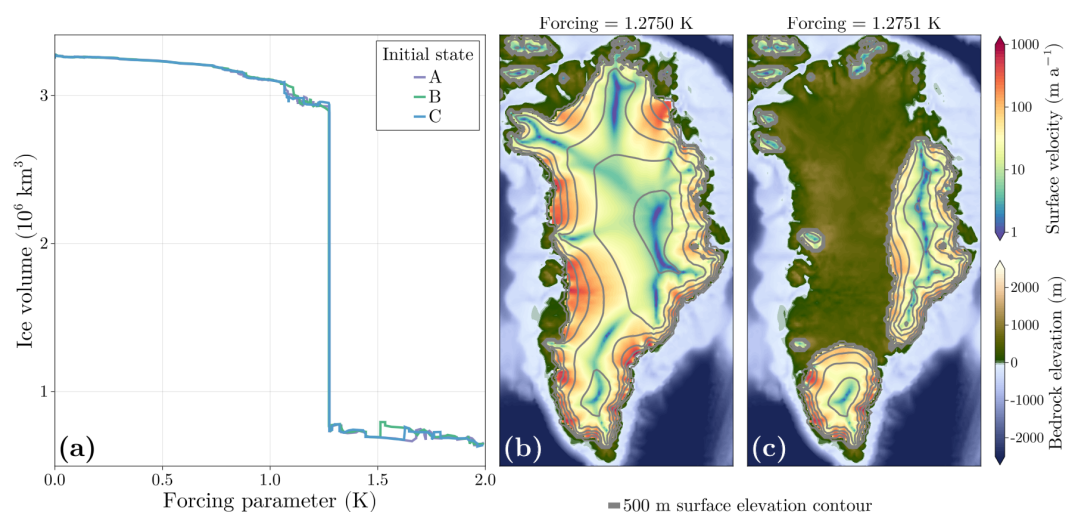


Figure 2. (a): Equilibrium ice volume of the GrIS as a function of the applied regional summer temperature anomaly in parameter space to estimate the tipping value for initial states A to C. (b): Ice-sheet before tipping. (c): Ice-sheet after tipping.

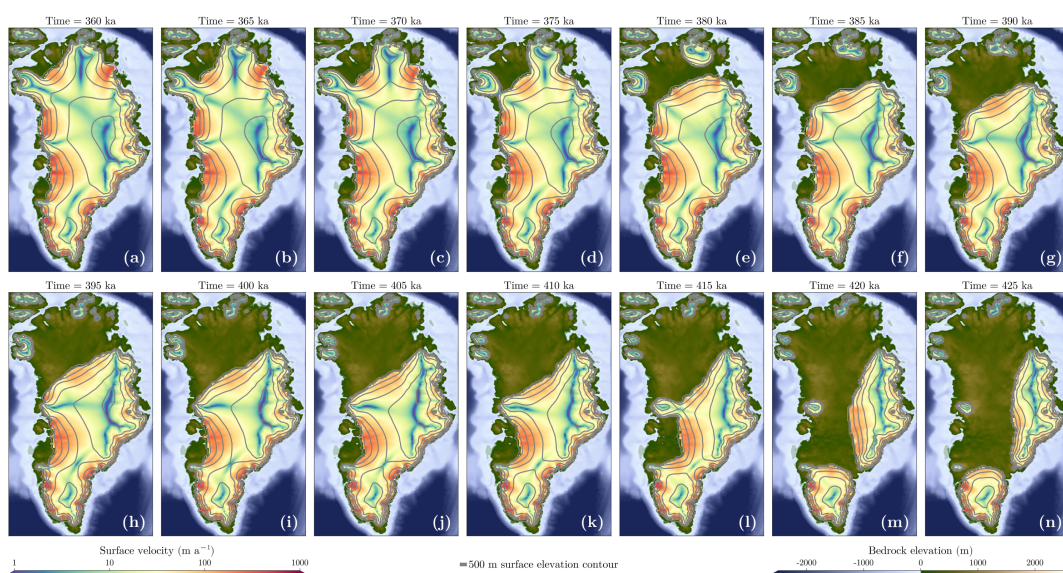


Figure 3. Ice extent and velocities during the tipping event at a fixed forcing value of +1.275 K.



3.2 Ramping experiments

Since the tipping point is located at +1.275 K, the maximal forcing of the ramping experiments are chosen as +1.00, 1.05, 1.10, 1.15, 1.20, and 1.25 K. A value of +1.30 K past the tipping point is also included to confirm that tipping does indeed always occur when forced past +1.275 K. The forcing increases linearly at a rate of 10^{-1} , 10^{-2} , 10^{-3} , 10^{-4} , or 10^{-5} K a⁻¹, up to
 130 one of the seven maximal forcing values noted previously. The time series of the forcing is shown in Fig. 4. As each of these 120 ramping experiments is initialized from one of three states A, B and C, the entire ensemble consists of $7 \times 5 \times 3 = 105$ members.

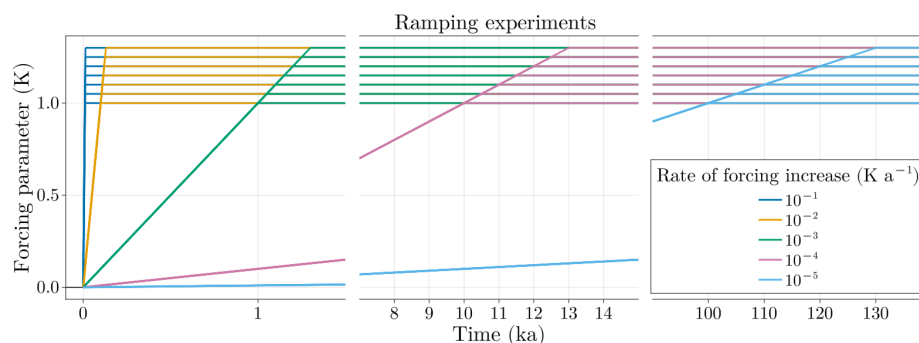


Figure 4. Time series of the forcing amplitude during the ramping experiments.

The simulations in Fig. 5 suggests rate-induced tipping. Tipping is observed for simulations forced to values lower than the critical value for b-tipping of +1.275 K, occurring between +1.10 and +1.25 K. Tipping also occurs for all of the simulations
 135 forced past the tipping point, that is, those forced to +1.30 K. What is absent, however, is some critical rate below which tipping does not occur, implying that r-tipping of the GrIS can occur even for very slow rates of forcing.

One prominent feature in this ensemble of simulations is the non-monotonicity in the tipping times. There is some agreement in tipping times among a given initial condition, as well as a dependence of the mean tipping time on the maximal forcing, being shorter for larger values. However, there is no clear relationship between the tipping time and the rate of forcing. Even
 140 for the same initial conditions, sometimes longer tipping times are achieved at lower forcing rates. For instance, for initial condition C at a forcing level of +1.25 K (panel (m) of Fig. 5), the trajectory forced at a rate of 10^{-2} K a⁻¹ tips around 300 ka, where the trajectory forced at slower rate of 10^{-3} K a⁻¹ tips earlier, around 100 ka.

In addition, tipping times for a maximum forcing of 1.30 K can be longer than those for 1.25 K. For example, for initial condition B and the slowest rate of 10^{-5} K a⁻¹, the tipping occurs around 250 ka for a forcing of +1.25 K and 400 ka for
 145 +1.30 K (panels (m) and (n) of Fig. 5, respectively). Finally, even for the same magnitude of forcing and rate of forcing, the tipping times are not consistent over initial conditions. For example, in panel (l) of Fig. 5, the simulation forced at a rate of 10^{-3} K a⁻¹ tip at 300, 350 and 250 ka for initial conditions A, B and C respectively. Overall, sensitive dependence on initial condition, indicative of chaos, appears to be affecting the outcome of the tipping.

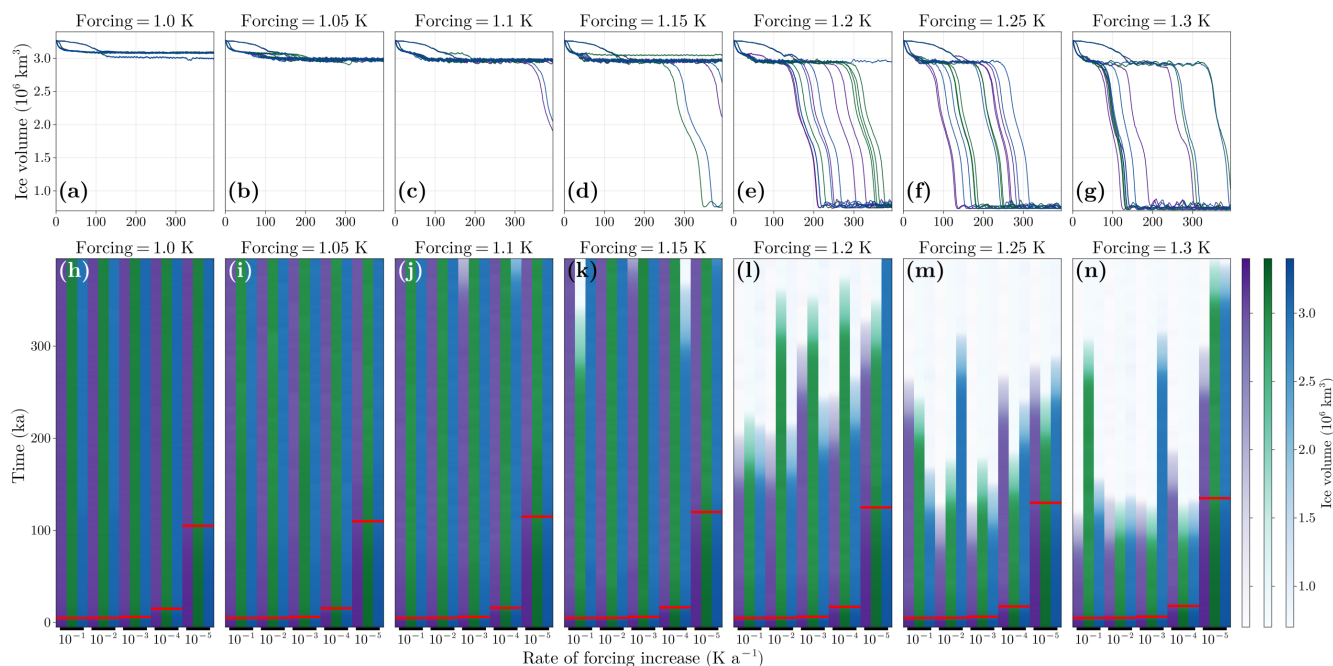


Figure 5. (a-g): Time series of the ice-sheet volume for all simulations at a given maximal forcing. (h-n): Time series of the ice volume for all of the simulations grouped by maximum forcing value. The initial state of each simulation is indicated by the different colours: purple for A, green for B and blue for C. For a given maximal forcing, the simulations are ordered along the bottom axis in decreasing rate of forcing, with the red line indicating the time where the forcing reaches its maximum.

While investigating the cause of these random tipping times, irregular oscillations in the ice sheet volume before tipping were observed. These oscillations can be isolated to a single region of the ice sheet: the northwest drainage basin, where the ice-sheet also begins its retreat during a tipping event. It is hypothesized that the random tipping times are linked to these irregular oscillations. An example of the oscillations for each maximal forcing is shown in Fig. 6. For all these simulations, there is an initial loss of mass during the first 50 - 80 ka of simulation time. Thereafter, for a maximal forcing of +1.00 K, there is a relatively small amount of variability around a steady ice volume of about $3.09 \times 10^6 \text{ km}^3$. For maximal forcing values between +1.05 and +1.15 K, the mean ice volume is lower, between 2.9 and $3.0 \times 10^6 \text{ km}^3$. The variability is also larger in both amplitude and period. Finally, the simulations for maximal forcing of +1.20 to +1.30 K in Fig. 6 retreat to a much smaller ice volume, representing a collapsed GrIS as seen in Fig. 2.c.

3.3 Spatial and temporal behaviour of the oscillations

Two simulations at a forcing of +1.00 1.05 K are compared, as this represents the onset of the large-amplitude variability seen in Fig. 6. Further examination of the oscillations show they are a result of two ice streams that alternate between periods of

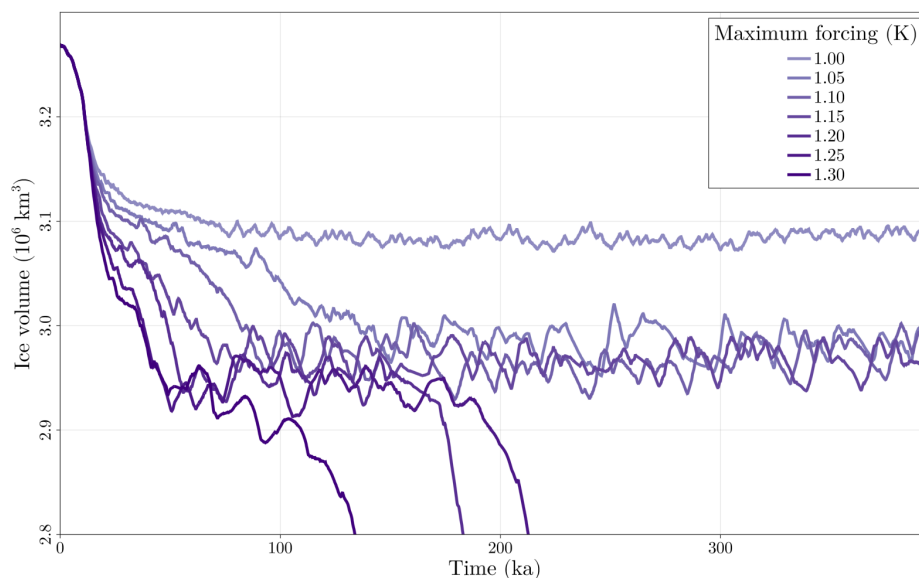


Figure 6. Time series of ice volume for simulations from Fig. 5 for initial condition A, rate of warming 10^{-4} K a^{-1} , and a range of maximal forcing values.

stagnant and rapid basal sliding. These are the Humboldt and Petermann glaciers, which lie in close proximity to each other on the northwestern ice-sheet edge. These glaciers are both regions of fast-flowing ice (Carr et al., 2015; Ehrenfeucht et al., 2023; Hillebrand et al., 2022) and behave as ice streams in the model simulations. In the model, ice streams can be identified by grounded ice with a significant basal velocity.

165 The first difference to be seen is the extent of the ice sheet in this region. For a forcing of +1.00 K, the ice-sheet margin is such that the Humboldt ice stream (HIS) is marine-terminating, with the Petermann ice stream (PIS) covering the Petermann fjord. The ice sheet in this case is termed ‘unretreated’. In the simulation with a forcing of +1.05 K, the ice sheet extent is much reduced. From the mean ice-thickness profiles, the ice margin is almost 100 km further inland (panels a, c, d and f of Fig. 7). The HIS is no longer connected to the ocean, although the PIS terminates at the Petermann fjord. We refer to this as
170 the ‘retreated’ configuration, with the two separate ice streams being designated the retreated HIS and retreated PIS.

The temporal behaviour of the two ice sheet extents is compared by taking the spatial mean in two grid boxes, one containing the PIS/retreated PIS and the other the HIS/retreated HIS, as seen in panels (a) and (j) of Fig. 8. For the unretreated case, the basal velocities in the two different ice streams behave quite differently. The PIS is in a state of steady flow of around 100 m a^{-1} , facilitated by a constant basal water layer thickness. The HIS, in contrast, alternates between near zero basal movement
175 and sliding velocities of 100 m a^{-1} . The periods of stagnation are due to an increase of basal friction because of a reduction in the water content of the till due to freezing or drainage. While the basal velocities are minimal, the ice thickness increases, establishing a ‘build up’ phase. The subsequent loss of mass due to rapid ice streaming is a ‘surge’ phase. The period of these

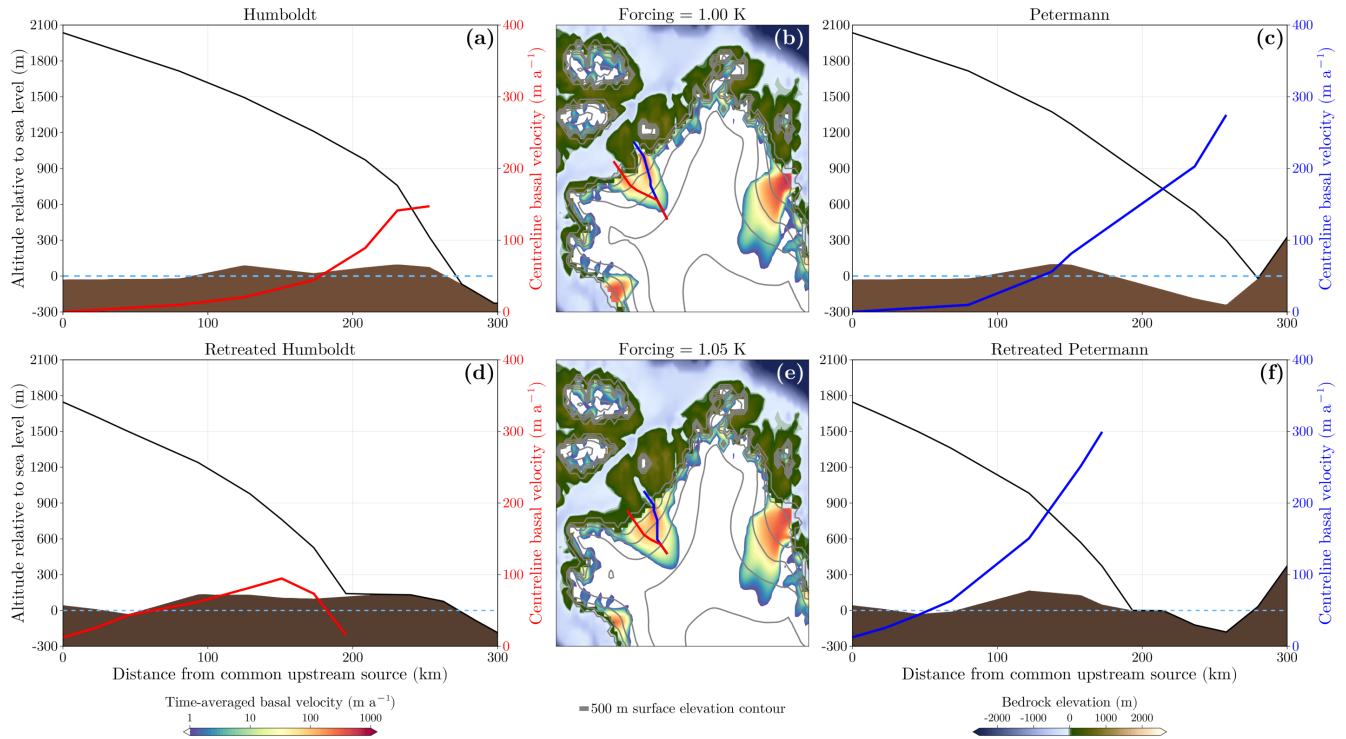


Figure 7. (a), (c): Centreline ice-thickness profile (black) and basal velocities along the centreline for the HIS and PIS. (d), (f): same as (a), (c) but for the retreated HIS and retreated PIS. (b), (e): time-averaged basal velocity field. The lines perpendicular to the grey height contours are the ice-stream centrelines for Humboldt (red) and Petermann (blue).

oscillations varies between approximately 5 and 9 ka. This steady cycle of mass gain during the build-up phase and loss during the surge results in an oscillation in mean ice thickness between 100 and 200 metres. The PIS also shows a smaller alternation in ice thickness with a similar temporal pattern while maintaining constant ice-stream flow, suggesting the thickness variations are influenced by the oscillations of the nearby HIS.

In the retreated configuration, the oscillations of ice thickness and basal velocity have larger amplitude and periodicity, as mentioned previously. While the exact location of the retreated PIS and retreated HIS differs slightly in all the simulations showing oscillations, their existence is robust among the ensemble. In contrast to the PIS, the retreated PIS is no longer in a steady-flow state and instead displays the same build-up/surge variability as the HIS and retreated HIS.

Two broad patterns for the oscillations of the retreated ice extent emerge. The first is one of a long, asymmetric build-up and surge event. An example is seen around 225 to 260 ka in panels c, e, g and i of Fig. 8. While the basal velocity in retreated PIS switches abruptly between the build-up and surge phases, the increase of the basal velocity in the retreated HIS is gradual. This slows the mass loss until a point where the basal water layer thickness rapidly decreases in both ice streams when the ice thickness reaches its minimum. The second pattern is that of short oscillations with a period of around 8 ka. These are seen

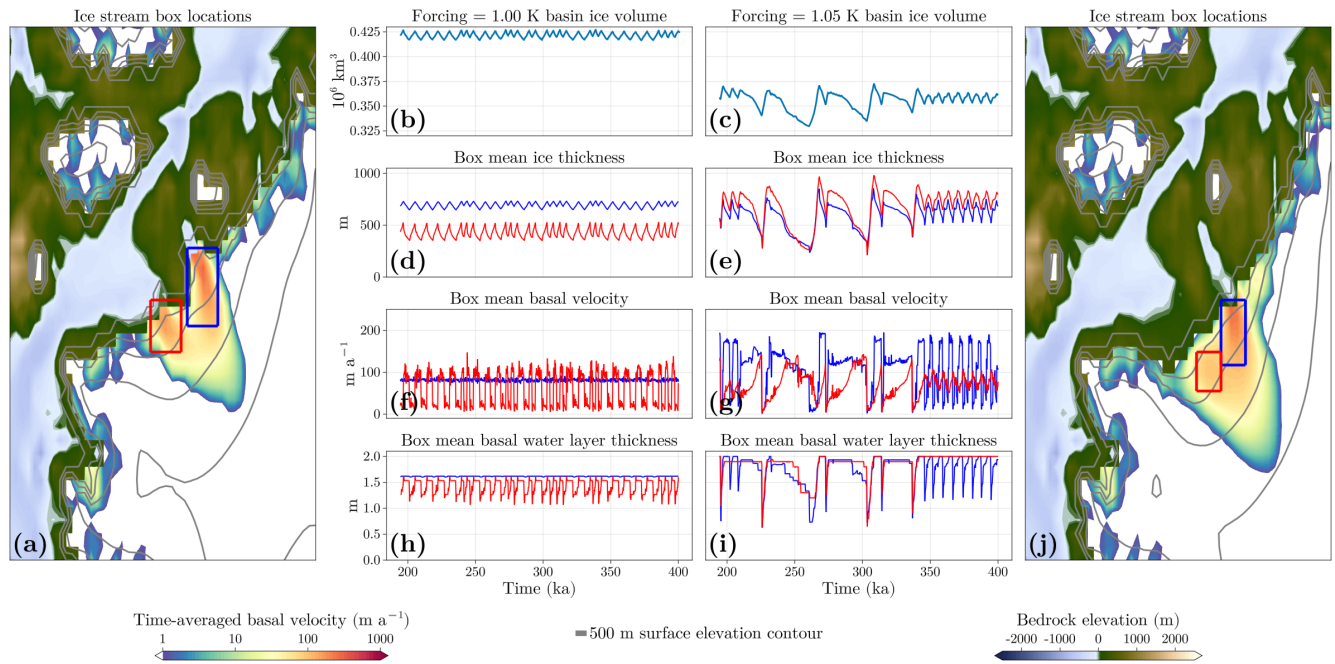


Figure 8. (a), (j): Location of the PIS/retrated PIS (blue) and HIS/retrated HIS (red) ice-stream boxes superimposed over the temporal average of the basal velocity during the oscillations of the unretrated (a) and retrated (j) configurations. (b-i): Time series of basin ice volume, mean ice thickness, basal velocity, and basal water content in the ice-stream boxes in the unretrated (d, b, f, h) and retrated (c, e, g, i) configurations.

in the last 60 ka of the time series in the panels c, e, g and i of Fig. 8. The basal velocity in retrated PIS abruptly switches between maximal and minimal, with corresponding drops in basal water-layer thickness when the velocity is near zero. In retrated HIS, the till remains saturated with water. However, the basal velocity and thereby the flow is not steady. It increases during the surge and decreases during the buildup of the nearby retrated PIS. This indicates an influence of the retrated PIS on the retrated HIS. The magnitude of ice-thickness change during this pattern is not as large as for build-up and surge variability, being around tens of metres per year in the spatial mean.

Thus the distinguishing factor between the two patterns is that during the short oscillations, retrated PIS is in a build-up/surge mode and retrated HIS has a constant till saturation associated with steady flow but experiences small oscillations due to the retrated PIS. On the other hand, both retrated HIS and retrated PIS are in the build-up/surge mode during the longer-period events. Additional to these modes, in some simulations with these oscillations there is occasionally a period where both retrated HIS and retrated PIS are in a steady flow state with intermediate mean basal velocities of around 100 m a^{-1} , with an associated minimum in the ice volume which may last tens of thousands of years.



3.4 Removal of the oscillations

To assess whether the lack of predictability of the tipping is due to ice-stream oscillations or otherwise due to other factors, we change the parameterization of the ice streams to eliminate their ability to oscillate and investigate the consequences. As described previously, the ice-stream oscillations are surges in the basal velocity of the ice stream due to the thermomechanical coupling at the base of the ice sheet. To remove the oscillations but maintain the ice stream, the basal velocities in the region of interest need to be lower but non-zero. For lower basal velocities, the mass lost due to streaming is closer to the accumulation rate, bringing the ice stream to a steady flow state (Robel et al., 2013). To achieve this, the value of δ in Eq. 3 is increased. This raises the minimal effective pressure (Bueler and van Pelt, 2015) and thereby increases the basal frictional stress.

Simulations with the original value of $\delta = 0.02$ as well as increasing values of δ to 0.04 and 0.10 are shown in Fig. 9. As δ is increased, we note an increase in the oscillatory period until the oscillations disappear completely. As this value affects ice streams across the entire ice sheet, the tipping points for each of these parameter values is different. Specifically, the tipping point increases as δ increases, as the ice sheet is losing less mass due to lower ice stream velocities.

For $\delta = 0.02$, all (no) simulations with the strongest (weakest) forcing tip, but for intermediate maximum forcing values the tipping times do not decrease monotonically with the forcing rates. For a large enough value of $\delta=0.1$, the ice-stream oscillations disappear and the tipping time for a maximal forcing of +2.10 K occurs at approximately the same time for each rate. That is, the dependency on the forcing rates disappears and the tipping is much more predictable. This suggests that the ice-stream oscillations introduce a delay in the tipping.

4 Discussion

4.1 Ice-stream oscillations

Ice streams not only represent a mechanism of rapid mass loss in ice sheets, but have also been shown to be a source of internal periodic variability in models. Periodic behaviour of ice masses can be seen in glaciers that are confined to some topographical valley and/or have a basal slope, see for example Budd (1975); Kamb et al. (1985); Clarke (1987). Their reduced spatial extent also means their periodic behaviour is on a much shorter time scale of decades to centuries and thus directly observable. Models show that ice sheets and ice streams, similar to valley glaciers, can also exhibit oscillatory behaviour under the right conditions.

Studies of oscillatory behaviour in ice sheets include parameterized models (Oerlemans, 1983; Fowler and Johnson, 1996; Payne, 1995; Robel et al., 2013) and comprehensive ice-sheet models with both idealized geometries (Calov et al., 2010; Van Pelt and Oerlemans, 2012; Feldmann and Levermann, 2017) and realistic topographies (Papa et al., 2006; Roberts et al., 2016; Schannwell et al., 2023). Additionally, some studies include a coupling to additional components of the climate system (Calov et al., 2002; Ziemen et al., 2019). Similarities between the oscillations seen in this paper and those observed in paleoclimate modelling studies are discussed in Appendix A.

Common to these studies is the use of a single initial state for a given combination of parameters rather than an ensemble. The use of an ensemble of states for investigating the evolution of an ice-sheet model is not too common, appearing in the

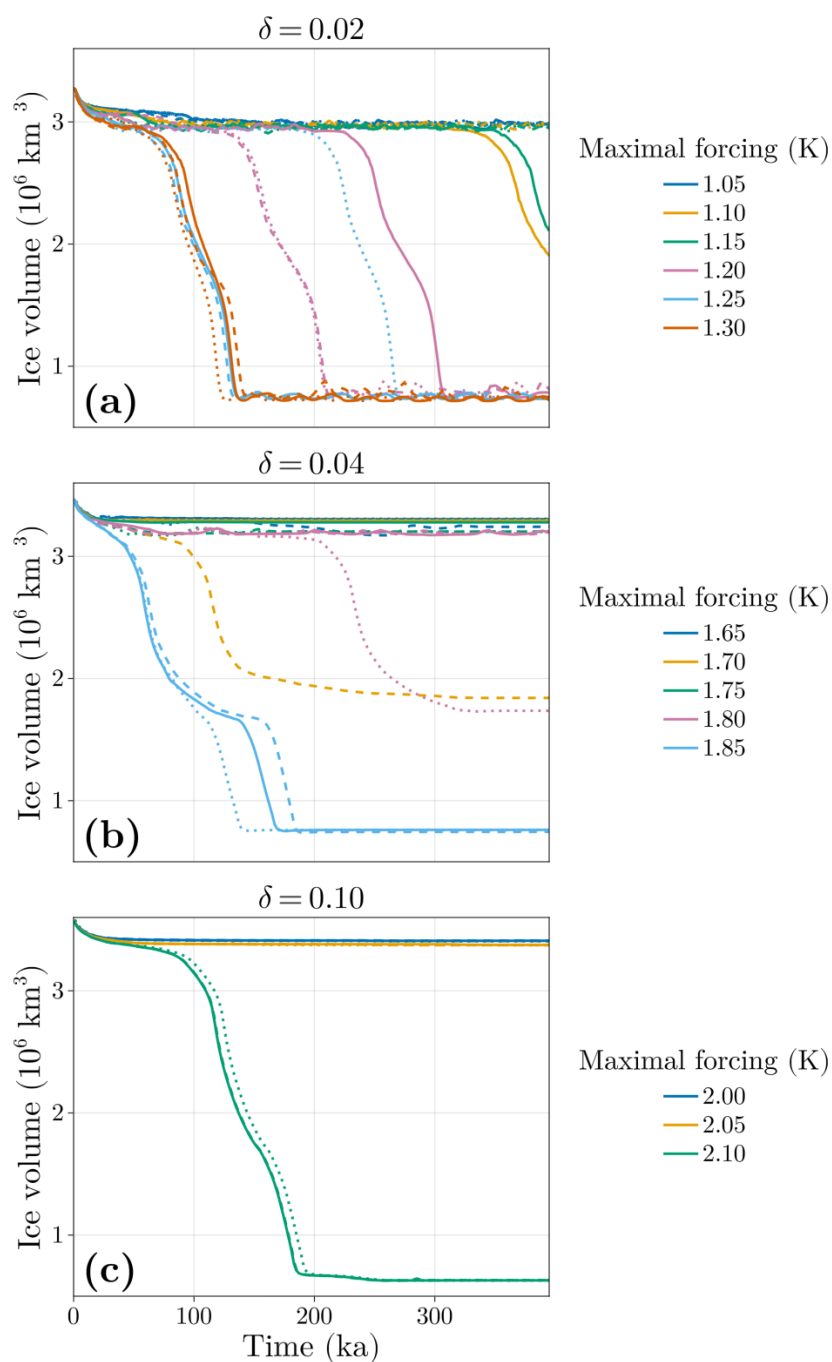


Figure 9. Time series of the ice sheet volume for increasing δ . For each value of δ , a range of forcing magnitudes at three rates starting from initial state A were applied: 10^{-1} (dotted lines), 10^{-2} (dashed lines) and 10^{-3} (solid lines) K a^{-1} .



235 studies of Tsai et al. (2017) and Verjans et al. (2025) to be able to account for the variability of the atmosphere and ocean when forcing the ice sheet. This is distinct to the results of this study, where the model is not coupled to an external climate beyond a simple, deterministic diffusive energy and moisture balance atmosphere and thus the variability is internal to the ice sheet itself. As a result of using an ensemble, we see simulations at a given forcing magnitude exhibit significant deviations from each other, indicating a sensitive dependence on the initial state which is a hallmark of a chaotic mode of internal variability.

240 The chaotic variability has an undeniable effect on the tipping behaviour. In particular, the unpredictable tipping times can be explained as being due to *chaotic transients*, which are described in Appendix B. Whether the chaos is a genuine physical phenomenon or simply a result of parameterization is under contention and will require further investigation. As variability of this type has been reported in many other ice-sheet modelling studies, its existence is not entirely unfounded. What is unique to this study is the period and amplitude of the oscillations in Greenland, as well as its switching between two different modes

245 due to a coupling of nearby ice streams. While oscillations in the GrIS ice volume have been reported in the modelling study of Zeitz et al. (2022), the period and amplitude of those oscillations are an order of magnitude higher than what is seen in the present work. This is due to the fact that glacial isostatic adjustment, which acts on a longer timescale than the melt-elevation feedback, plays a much larger role in their model.

4.2 R-tipping of the GrIS

250 Accelerating mass loss is typically seen in marine-terminating outlet glaciers due to their sensitivity to oceanic forcing (Howat et al., 2008; Krabill et al., 2004; Rignot and Kanagaratnam, 2006), suggesting rate-induced effects may be more prevalent in these areas. However, they are topographically confined and their impact may be limited under greater forcing (Joughin et al., 2010). For this reason, future loss due to negative surface mass balance forced by increasing atmospheric temperatures could outweigh that of ice-sheet dynamics (Bevis et al., 2019; Enderlin et al., 2014). The ice extent shown in Fig. 3 indicates that the

255 mass loss does not start in regions with many marine-terminating outlet glaciers, specifically the southeast (Van Den Broeke et al., 2009). In fact, many remain after the tipping has completed. This indicates that the possibility of r-tipping of the GrIS primarily by oceanic forcing may not be relevant.

The remainder of the ice sheet interacts predominantly with the atmosphere, and the mass loss occurs either through surface melt or dynamically through ice streams which may not necessarily be marine-terminating. The question of whether the large-

260 scale mass loss of the GrIS can be influenced by the sensitivity of these fast-moving ice streams to the rate of atmospheric warming is greatly obscured by the chaotic variability seen in the model. The simulations indicate that the tipping behaviour is affected by the rate of forcing but in a non-monotonic manner. There is no clear critical forcing rate for which r-tipping occurs, at least not for a rate faster than one Kelvin of warming over 100 ka. However, the long tipping times are not explained by non-monotonic r-tipping, as we would expect any tipping events to occur at roughly the same time at a given forcing

265 magnitude. That is, it is valid to claim that r-tipping does indeed occur since the final state of the GrIS depends on the rate of forcing in some way, but it is not the typical r-tipping as understood in simple non-chaotic systems. It is rather related to sensitive dependence on an initial state rather than any critical rate of forcing, with the different rates of forcing essentially being perturbations of the initial state, resulting in trajectories with unpredictable behaviour.



4.3 Removal of the oscillations

270 Removing the oscillations by increasing δ makes the tipping more predictable. At a value of $\delta = 0.1$, the tipping occurs at approximately the same time for both the fast and slow rates of forcing increase. This is in contrast to the simulations with $\delta = 0.02$, where oscillations are present and the tipping at a given maximal forcing can vary by tens to hundreds of thousands of years depending on the rate and in a non-monotonic manner. This corroborates the hypothesis that the oscillations cause the delay in tipping. For an intermediate value of $\delta = 0.04$, tipping to an ice-free state only occurs for the largest forcing magnitude
275 of +1.85 K. Interestingly, two simulations at lower forcing magnitudes see a tipping to an intermediate ice-sheet state. Such a state has been seen before in studies such as Ridley et al. (2010) and Robinson et al. (2012), but is not explored further in the present paper.

Increasing δ also reveals some interesting interplay between the parameterization that allows for the oscillations and the tipping. As increasing δ decreases the ice-stream velocity, the ice sheet loses less mass dynamically and thus the forcing
280 magnitude required for tipping increases. However, the tipping is now no longer delayed by the oscillations. Since the lifetime of the transients can be upwards of 100 ka, it may be the case that the tipping occurs later for a lower forcing value. Thus the oscillations simultaneously serve to lower the value of the tipping point as well as to increase the time before tipping occurs.

5 Conclusions and future work

Setting out to identify whether the GrIS is susceptible to r-tipping, we performed warming experiments at different rates using
285 a comprehensive ice-sheet model. In the course of this line of investigation, it was discovered that the coupled model exhibits a mode of variability that has heretofore not been observed in models of the GrIS. This is presumably because, at least for our model, they only exist for a very small range of external temperature forcing between +1.05 and +1.30 K.

This variability appears in the form of oscillations of ice streams in the present-day GrIS due to thermomechanical coupling at the base of the ice. Warming of the ice sheet causes an initial retreat of the ice extent in the northwest region, resulting in
290 the Petermann and Humboldt glaciers entering a configuration where they experience build-up/surge variability. Due to their proximity, they influence each other and the resulting pattern is chaotic. Since the tipping of the ice sheet begins in the region where these ice streams are found, their presence delays the tipping of the ice sheet to an ice-free state.

The conclusions are limited by the amounts and types of simulations conducted. An obvious next step is to repeat experiments using a different grid size to observe the dependence, if any, of these oscillations on the model domain. A full
295 investigation of the phase space and the basins of attraction in the parameter range around the tipping would give a much clearer picture on when the tipping may occur, or if there are multiple closer steady states before a larger tipping. Additionally, an edge-tracking algorithm (Lucarini and Bódai, 2017; Mehling et al., 2024; Börner et al., 2025) can be used to approximate the chaotic non-attracting set, even for a ghost attractor. This can be used to identify whether it is such a ghost attractor, or else a chaotic saddle.

300 In connection with other elements of the climate system, the oscillations themselves on a shorter time scale are worth studying. For example, they may represent a periodic freshwater forcing condition on the AMOC. If the retreated configuration



where oscillations occur is considered as a separate state to the current ice-covered GrIS, r-tipping onto this attractor may be investigated.

305 The implications of chaotic transients on anthropogenic climate change in this context is phenomenological rather than sociologically relevant due to the long time scales. Long tipping times might erroneously suggest that the GrIS is stable, although it eventually tips when keeping the forcing parameter constant. On the other hand, these long transients allow for overshooting of the tipping point, whereafter the forcing parameter may still be reduced in time to prevent the tipping.

Code availability

310 The source code for Yelmo and REMBO can be found at <https://github.com/palma-ice/yelmo> and <https://github.com/alex-robinson/rembo1>, respectively.

Author contribution

315 **KK:** Conceptualization, Investigation, Visualization, Writing (original draft). **MM:** Conceptualization, Methodology, Software, Writing (review and editing) **AR:** Conceptualization, Methodology, Software, Writing (review and editing) **JA-S:** Conceptualization, Methodology, Software, Writing (review and editing) **JS-J:** Conceptualization, Methodology, Software, Writing (review and editing) **PD:** Conceptualization, Writing (review and editing)

Competing interests

The authors declare that they have no known competing financial interests or personal relationships that could have appeared to influence the work reported in this paper.

Acknowledgments

320 KK would like to thank Reyk Börner, Oliver Mehling, and Johannes Lohmann for valuable discussions.

Financial support

325 This project has received funding from the European Union's Horizon 2020 research and innovation programme under the Marie Skłodowska-Curie Innovative Training Network CriticalEarth, grant agreement no. 956170. This is a contribution to the European Union's Horizon 2020 research and innovation programme ClimTip, grant agreement no. 101137601. Alexander Robinson received funding from the European Research Council (ERC Consolidator grant, FORCLIMA, grant no. 101044247).



Appendix A: Comparison to oscillations of the LIS

Large-scale oscillations of ice streams were first proposed as the reason for Heinrich events (HEs) during the last glacial period (LGP) (Heinrich, 1988; Broecker et al., 1992; MacAyeal, 1993), but these events might be caused instead by external forcing (Alvarez-Solas et al., 2013; Bassis et al., 2017). While the variability of the oscillations seen in this study seems similar to the build-up/surge variability seen in most simulations of HEs in the Laurentide ice sheet (LIS) of the LGM (Calov et al., 2002; Papa et al., 2006; Roberts et al., 2016; Ziemen et al., 2019; Schannwell et al., 2023), they do not match exactly. Most notably, the Hudson ice stream in those studies displays a more gradual increase in ice volume followed by a sudden surge. This is in contrast to the pattern in the retreated HIS and retreated PIS in this experiment, where the build-up is either over the same time period (in the case of the short oscillations) or faster (in the case of the longer asymmetric events) than the subsequent surge. Additionally, in the latter case, the ice loss accelerates over time, rather than being maximal at the beginning of the surge. It may be the case that the variability seen in the GrIS, while having the same physical mechanism of thermo-mechanical coupling, may have a source additional of variability, i.e. the spatial interaction of the retreated PIS and retreated HIS, that causes it to behave differently from these experiments of a single oscillating ice stream.

Common to ice-sheet model simulations of the LIS are oscillations in ice-sheet volume that sometimes show quasiperiodicity or seemingly chaotic behaviour. It would be expected that, due to the large spatial extent of the system and the complex basal topography, the oscillations would not have a near-constant period. Even in the idealized geometry of Calov et al. (2010) there is spontaneous spatial asymmetry that leads to inconsistent oscillatory frequency. Such irregular variability is of special importance when studying the tipping behaviour of a system. Still, without an ensemble of simulations starting from similar initial conditions, it is unknown how irregular the variability seen in these studies is.

Appendix B: Link to nonlinear dynamics

B1 Chaotic transients

Systems that experience chaotic variability have long transients with lifetimes of indeterminate length, and these are hence called chaotic transients (Lai and Tél, 2011). Specifically, the lifetime of any chaotic transient depends sensitively on its initial condition, but the lifetimes of an ensemble are exponentially distributed. These chaotic transients are due to the existence of chaotic non-attracting sets, the most relevant being chaotic ‘ghost attractors’ and chaotic saddles. The distinction is important, as the ghost attractor exists in the monostable parameter regime, whereas the chaotic saddle exists in the bistable parameter regime.

A chaotic ghost attractor materializes as a result of a chaotic attractor undergoing a *boundary crisis* due to a continuously changing parameter (Grebogi et al., 1982), essentially a chaotic analogue of a saddle-node bifurcation. A trajectory that is forced beyond this crisis parameter value will remain around the ghost attractor for some time before eventually tipping, causing the chaotic transient. On the other hand, a chaotic saddle lies on the basin boundary that separates two co-existing attractors. It generates long-lived transients when a trajectory crosses this basin boundary, as solutions are captured by the



attracting manifolds of the saddle before eventually approaching one of the two attractors. Such a phenomenon in the context of r-tipping has been previously reported in a study by Lohmann and Ditlevsen (2021) for the Atlantic Meridional Overturning Circulation (AMOC). In their study, trajectories forced at different rates are brought close to the basin boundary between the stable ‘AMOC on’ state and the chaotic saddle that separates it from the stable ‘AMOC off’ state. As the basin boundary is fractal, differing rates may cause it to tip or not in a non-monotonic way. For a chaotic saddle, the mean lifetime of chaotic transients scales with the fractal dimension of the saddle (Hunt et al., 1996; Mehling et al., 2024; Sweet and Ott, 2000).

Due to being a transient simulation, the AQEF itself may exhibit a chaotic transient. The biggest evidence for this is comparing the simulations ramped to +1.25 K and 1.30 K. If the oscillations are due to crossing a chaotic saddle before the tipping point of 1.275 K is reached (i.e those simulations for +1.25 K), then they must be qualitatively different from the ghost attractor generated by a boundary crisis after the boundary crisis (i.e those for +1.30 K), as the chaotic saddle only exists in the bistable parameter regime and the ghost attractor only exists in the monostable parameter regime. However, the trajectories at both forcing values occupy the same regions of phase space before tipping, implying that they are the same type of chaotic transient. This implies that the bifurcation does not occur between +1.25 K and 1.30 K. Similar reasoning can be applied to all parameter values that result in tipping. Thus, the bifurcation point is either between +1.05 K and 1.10 K and all transients are due to a ghost attractor, or the tipping point is larger than +1.30 K and all of the transients are due to an r-tipping through a chaotic saddle.

The behaviour of the chaotic transients in the present study more closely resembles those due to a boundary crisis than crossing a chaotic saddle. First, scaling laws indicate that the lifetime of the chaotic saddle, and thereby the tipping time, should increase as the maximal forcing approaches the bifurcation point from the left (Mehling et al., 2024). In contrast, the mean lifetime of the chaotic transients scales with the magnitude of the parameter past the crisis value (Grebogi et al., 1986),

$$\langle \tau \rangle \sim (p - p_c)^{-\gamma}, \quad (\text{B1})$$

which mirrors the pattern seen in the tipping times in Fig. 5. Secondly, if r-tipping was present, we may expect to see tipping not occur below some critical rate.

B2 Transient lifetime for a forcing value of 1.05 K

The state of the system at a forcing level of +1.05 K is of interest since it is on the boundary between more predictable patterns and the irregular oscillations of the chaotic transients. None of the simulations at this forcing value tip to an ice free state after 400 ka of model time, although they exhibit the same variability as those that do tip. In this parameter range, the system may either be either on a chaotic attractor, or otherwise a chaotic transient with a lifetime much longer than 400 ka.

Using the mean lifetime of the simulations that tip to an ice-free state, the critical exponent in equation B1 can be estimated. Using a maximum likelihood estimation to fit them to an exponential distribution results in a critical exponent of around $\gamma \sim 9.959$. Using this, the mean tipping time for a trajectory with a maximal forcing of +1.05 K is around 511 ka, which is indeed longer than the 400 ka simulation run time.

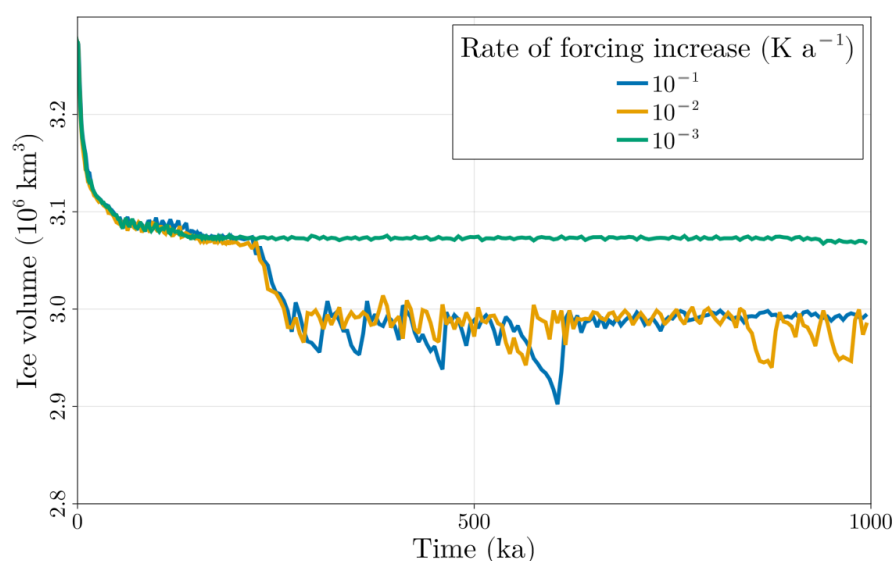


Figure B1. Simulations to 1 Ma for a maximal forcing of +1.05 K at three different rates. This simulation time is estimated to be longer than the mean lifetime of a chaotic transient at this forcing value. The temporal resolution of the output of these simulations for the final 800 ka is 5 ka, in comparison to the 200 a timestep the simulations in Figs. 5, 6 and 8.

390 A few additional simulations at this forcing level were done going to 1 Ma and are seen in Fig. B1. None of these simulations tip, suggesting that they are not chaotic transients but rather motion on a chaotic attractor, and the ice sheet has a genuine chaotic attractor at this parameter value. This further strengthens the argument that the chaotic transients are generated by a boundary crisis, as the resulting ghost attractor is qualitatively similar to the chaotic attractor that exists before the crisis Lai and Tél (2011).

395 **B3 Intermediate tipping**

Within the simulation ensemble, there are a few ‘anomalous’ runs that do not behave as expected. There are two such types: first, for a forcing level of +1.00 K, one simulation ends up in the retreated configuration with ice-volume variability similar to but slightly smaller in magnitude than those of larger forcing values, as seen in Fig. B2. This might suggest the chaotic attractor associated with the ice-stream oscillations also exists for lower forcing values, albeit with a smaller basin of attraction and thus it has a lower probability of being reached.

Second, there is a simulation with a maximal forcing of +1.15 K that remains in the unretreated configuration. That is, for larger forcing values the less chaotic attractor remains at a diminished size. The 1 Ma simulations for a maximal forcing of

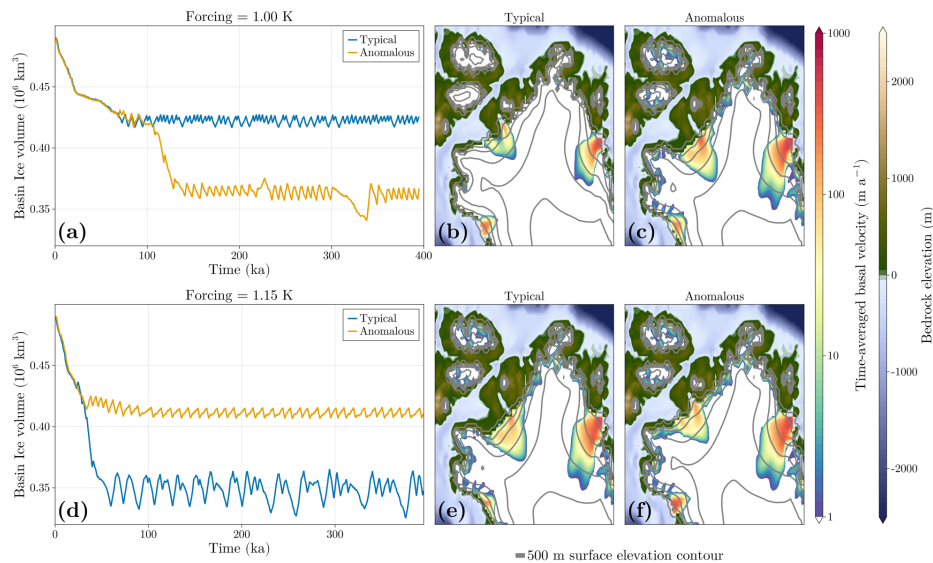


Figure B2. (a): Time series and mean ice thickness for typical and anomalous model trajectories at a forcing of +1.00. (b): Ice sheet extent and time-averaged basal velocity fields of a typical trajectory. (c): Ice sheet extent and time-averaged basal velocity fields of the anomalous trajectory. (d-f): Same as (a-c) but for a forcing of +1.15 K.

+1.05 K in Fig. B1 also show the unretreated configuration is possible at this forcing value. This represents a complication in the analysis, since this parameter value is assumed to be associated the chaotic attractor or its ghost.

405 In this case, the structure of the attractors may be that there is intermediate tipping similar to Lohmann et al. (2024). This would imply that around a forcing value of +1.00 to +1.05 K, there are two attractors for the ice-covered state, corresponding to the retreated and unretreated configurations. The attractor for the retreated GrIS experiences a boundary crisis between +1.05 and +1.10 K, with corresponding chaotic transients remaining on the associated ghost attractor. On the other hand, the attractor of the unretreated GrIS experiences a bifurcation at a forcing value slightly larger than +1.15 K. This scenario could then have
410 genuine r-tipping onto either the unretreated or retreated configurations, the latter of which experiences an earlier tipping to an ice-free state, resulting in an indirect r-tipping to the ice-free state. The basin boundary between the two ice-covered attractors could be fractal, leading to nearby initial conditions approaching one or the other (McDonald et al., 1985).



References

- Albrecht, T., Winkelmann, R., and Levermann, A.: Glacial-cycle simulations of the Antarctic Ice Sheet with the Parallel Ice Sheet Model (PISM) – Part 2: Parameter ensemble analysis, *The Cryosphere*, 14, 633–656, <https://doi.org/10.5194/tc-14-633-2020>, publisher: Copernicus GmbH, 2020.
- Alvarez-Solas, J., Robinson, A., Montoya, M., and Ritz, C.: Iceberg discharges of the last glacial period driven by oceanic circulation changes, *Proceedings of the National Academy of Sciences*, 110, 16 350–16 354, <https://doi.org/10.1073/pnas.1306622110>, 2013.
- Armstrong McKay, D. I., Staal, A., Abrams, J. F., Winkelmann, R., Sakschewski, B., Loriani, S., Fetzer, I., Cornell, S. E., Rockström, J., and Lenton, T. M.: Exceeding 1.5°C global warming could trigger multiple climate tipping points, *Science (New York, N.Y.)*, 377, eabn7950, <https://doi.org/10.1126/science.abn7950>, 2022.
- Ashwin, P., Wieczorek, S., Vitolo, R., and Cox, P.: Tipping points in open systems: bifurcation, noise-induced and rate-dependent examples in the climate system, *Philosophical Transactions of the Royal Society A: Mathematical, Physical and Engineering Sciences*, 370, 1166–1184, <https://doi.org/10.1098/rsta.2011.0306>, publisher: Royal Society, 2012.
- Bassis, J. N., Petersen, S. V., and Mac Cathles, L.: Heinrich events triggered by ocean forcing and modulated by isostatic adjustment, *Nature*, 542, 332–334, <https://doi.org/10.1038/nature21069>, publisher: Nature Publishing Group, 2017.
- Bevis, M., Harig, C., Khan, S. A., Brown, A., Simons, F. J., Willis, M., Fettweis, X., Van Den Broeke, M. R., Madsen, F. B., Kendrick, E., Caccamise, D. J., Van Dam, T., Knudsen, P., and Nylen, T.: Accelerating changes in ice mass within Greenland, and the ice sheet’s sensitivity to atmospheric forcing, *Proceedings of the National Academy of Sciences*, 116, 1934–1939, <https://doi.org/10.1073/pnas.1806562116>, 2019.
- Blasco, J., Tabone, I., Moreno-Parada, D., Robinson, A., Alvarez-Solas, J., Pattyn, F., and Montoya, M.: Antarctic tipping points triggered by the mid-Pliocene warm climate, *Climate of the Past*, 20, 1919–1938, <https://doi.org/10.5194/cp-20-1919-2024>, publisher: Copernicus GmbH, 2024.
- Bochow, N., Poltronieri, A., Robinson, A., Montoya, M., Rypdal, M., and Boers, N.: Overshooting the critical threshold for the Greenland ice sheet, *Nature*, 622, 528–536, <https://doi.org/10.1038/s41586-023-06503-9>, number: 7983 Publisher: Nature Publishing Group, 2023.
- Broecker, W., Bond, G., Klas, M., Clark, E., and McManus, J.: Origin of the northern Atlantic’s Heinrich events, *Climate Dynamics*, 6, 265–273, <https://doi.org/10.1007/BF00193540>, 1992.
- Budd, W. F.: A First Simple Model for Periodically Self-Surging Glaciers, *Journal of Glaciology*, 14, 3–21, <https://doi.org/10.3189/S0022143000013344>, 1975.
- Bueler, E. and van Pelt, W.: Mass-conserving subglacial hydrology in the Parallel Ice Sheet Model version 0.6, *Geoscientific Model Development*, 8, 1613–1635, <https://doi.org/10.5194/gmd-8-1613-2015>, publisher: Copernicus GmbH, 2015.
- Börner, R., Mehling, O., Hardenberg, J. v., and Lucarini, V.: Boundary crisis and long transients of the Atlantic overturning circulation mediated by an edge state, <https://doi.org/10.48550/arXiv.2504.20002>, arXiv:2504.20002 [nlin], 2025.
- Calov, R., Ganopolski, A., Petoukhov, V., Claussen, M., and Greve, R.: Large-scale instabilities of the Laurentide ice sheet simulated in a fully coupled climate-system model, *Geophysical Research Letters*, 29, <https://doi.org/10.1029/2002GL016078>, 2002.
- Calov, R., Greve, R., Abe-Ouchi, A., Bueler, E., Huybrechts, P., Johnson, J. V., Pattyn, F., Pollard, D., Ritz, C., Saito, F., and Tarasov, L.: Results from the Ice-Sheet Model Intercomparison Project–Heinrich Event Intercomparison (ISMIP HEINO), *Journal of Glaciology*, 56, 371–383, <https://doi.org/10.3189/002214310792447789>, 2010.



- Carr, J., Vieli, A., Stokes, C., Jamieson, S., Palmer, S., Christoffersen, P., Dowdeswell, J., Nick, F., Blankenship, D., and Young, D.: Basal topographic controls on rapid retreat of Humboldt Glacier, northern Greenland, *Journal of Glaciology*, 61, 137–150, <https://doi.org/10.3189/2015JoG14J128>, 2015.
- Clarke, G. K. C.: Fast glacier flow: Ice streams, surging, and tidewater glaciers, *Journal of Geophysical Research: Solid Earth*, 92, 8835–8841, <https://doi.org/10.1029/JB092iB09p08835>, 1987.
- Ehrenfeucht, S., Morlighem, M., Rignot, E., Dow, C. F., and Mouginot, J.: Seasonal Acceleration of Petermann Glacier, Greenland, From Changes in Subglacial Hydrology, *Geophysical Research Letters*, 50, e2022GL098009, <https://doi.org/10.1029/2022GL098009>, _eprint: <https://onlinelibrary.wiley.com/doi/pdf/10.1029/2022GL098009>, 2023.
- Enderlin, E. M., Howat, I. M., Jeong, S., Noh, M.-J., van Angelen, J. H., and van den Broeke, M. R.: An improved mass budget for the Greenland ice sheet, *Geophysical Research Letters*, 41, 866–872, <https://doi.org/10.1002/2013GL059010>, _eprint: <https://onlinelibrary.wiley.com/doi/pdf/10.1002/2013GL059010>, 2014.
- Feldmann, J. and Levermann, A.: From cyclic ice streaming to Heinrich-like events: the grow-and-surge instability in the Parallel Ice Sheet Model, *The Cryosphere*, 11, 1913–1932, <https://doi.org/10.5194/tc-11-1913-2017>, publisher: Copernicus GmbH, 2017.
- Feudel, U.: Rate-induced tipping in ecosystems and climate: the role of unstable states, basin boundaries and transient dynamics, *Nonlinear Processes in Geophysics*, 30, 481–502, <https://doi.org/10.5194/npg-30-481-2023>, publisher: Copernicus GmbH, 2023.
- Fowler, A. C. and Johnson, C.: Ice-sheet surging and ice-stream formation, *Annals of Glaciology*, 23, 68–73, <https://doi.org/10.3189/S0260305500013276>, 1996.
- Goldberg, D. N.: A variationally derived, depth-integrated approximation to a higher-order glaciological flow model, *Journal of Glaciology*, 57, 157–170, <https://doi.org/10.3189/002214311795306763>, publisher: International Glaciological Society, 2011.
- Grebogi, C., Ott, E., and Yorke, J. A.: Chaotic Attractors in Crisis, *Physical Review Letters*, 48, 1507–1510, <https://doi.org/10.1103/PhysRevLett.48.1507>, publisher: American Physical Society, 1982.
- Grebogi, C., Ott, E., and Yorke, J. A.: Critical Exponent of Chaotic Transients in Nonlinear Dynamical Systems, *Physical Review Letters*, 57, 1284–1287, <https://doi.org/10.1103/PhysRevLett.57.1284>, publisher: American Physical Society, 1986.
- Gregory, J. M., Huybrechts, P., and Raper, S. C. B.: Threatened loss of the Greenland ice-sheet, *Nature*, 428, 616–616, <https://doi.org/10.1038/428616a>, publisher: Nature Publishing Group, 2004.
- Gutiérrez-González, L., Robinson, A., Alvarez-Solas, J., Tabone, I., Swierczek-Jereczek, J., Moreno-Parada, D., and Montoya, M.: Hysteresis of the Greenland ice sheet from the Last Glacial Maximum to the future.
- Heinrich, H.: Origin and Consequences of Cyclic Ice Rafting in the Northeast Atlantic Ocean During the Past 130,000 Years, *Quaternary Research*, 29, 142–152, [https://doi.org/10.1016/0033-5894\(88\)90057-9](https://doi.org/10.1016/0033-5894(88)90057-9), 1988.
- Hillebrand, T. R., Hoffman, M. J., Perego, M., Price, S. F., and Howat, I. M.: The contribution of Humboldt Glacier, northern Greenland, to sea-level rise through 2100 constrained by recent observations of speedup and retreat, *The Cryosphere*, 16, 4679–4700, <https://doi.org/10.5194/tc-16-4679-2022>, publisher: Copernicus GmbH, 2022.
- Holland, D. M., Thomas, R. H., de Young, B., Ribergaard, M. H., and Lyberth, B.: Acceleration of Jakobshavn Isbræ triggered by warm subsurface ocean waters, *Nature Geoscience*, 1, 659–664, <https://doi.org/10.1038/ngeo316>, publisher: Nature Publishing Group, 2008.
- Howat, I. M., Joughin, I., Fahnestock, M., Smith, B. E., and Scambos, T. A.: Synchronous retreat and acceleration of southeast Greenland outlet glaciers 2000–06: ice dynamics and coupling to climate, *Journal of Glaciology*, 54, 646–660, <https://doi.org/10.3189/002214308786570908>, 2008.



- Hunt, B. R., Ott, E., and Yorke, J. A.: Fractal dimensions of chaotic saddles of dynamical systems, *Physical Review E*, 54, 4819–4823, <https://doi.org/10.1103/PhysRevE.54.4819>, 1996.
- Höning, D., Willeit, M., Calov, R., Klemann, V., Bagge, M., and Ganopolski, A.: Multistability and Transient Response of the Greenland Ice Sheet to Anthropogenic CO₂ Emissions, *Geophysical Research Letters*, 50, e2022GL101827, <https://doi.org/10.1029/2022GL101827>,
490 _eprint: <https://agupubs.onlinelibrary.wiley.com/doi/pdf/10.1029/2022GL101827>, 2023.
- Intergovernmental Panel On Climate Change (IPCC): Climate Change 2021 – The Physical Science Basis: Working Group I Contribution to the Sixth Assessment Report of the Intergovernmental Panel on Climate Change, Cambridge University Press, 1 edn., ISBN 978-1-00-915789-6, <https://doi.org/10.1017/9781009157896>, 2023.
- Joughin, I., Smith, B. E., Howat, I. M., Scambos, T., and Moon, T.: Greenland flow variability from ice-sheet-wide velocity mapping, *Journal*
495 *of Glaciology*, 56, 415–430, <https://doi.org/10.3189/002214310792447734>, 2010.
- Joughin, I., Smith, B. E., and Schoof, C. G.: Regularized Coulomb Friction Laws for Ice Sheet Sliding: Application to Pine Island Glacier, Antarctica, *Geophysical Research Letters*, 46, 4764–4771, <https://doi.org/10.1029/2019GL082526>, _eprint: <https://onlinelibrary.wiley.com/doi/pdf/10.1029/2019GL082526>, 2019.
- Kamb, B., Raymond, C. F., Harrison, W. D., Engelhardt, H., Echelmeyer, K. A., Humphrey, N., Brugman, M. M., and Pfeffer, T.: Glacier
500 Surge Mechanism: 1982–1983 Surge of Variegated Glacier, Alaska, *Science, New Series*, 227, 469–479, <http://www.jstor.org/stable/1694144>, 1985.
- Khan, S. A., Kjær, K. H., Bevis, M., Bamber, J. L., Wahr, J., Kjeldsen, K. K., Bjørk, A. A., Korsgaard, N. J., Stearns, L. A., Van Den Broeke, M. R., Liu, L., Larsen, N. K., and Muresan, I. S.: Sustained mass loss of the northeast Greenland ice sheet triggered by regional warming, *Nature Climate Change*, 4, 292–299, <https://doi.org/10.1038/nclimate2161>, 2014.
- 505 Krabill, W., Hanna, E., Huybrechts, P., Abdalati, W., Cappelen, J., Csatho, B., Frederick, E., Manizade, S., Martin, C., Sonntag, J., Swift, R., Thomas, R., and Yungel, J.: Greenland Ice Sheet: Increased coastal thinning, *Geophysical Research Letters*, 31, <https://doi.org/10.1029/2004GL021533>, _eprint: <https://onlinelibrary.wiley.com/doi/pdf/10.1029/2004GL021533>, 2004.
- Lai, Y.-C. and Tél, T.: Transient Chaos, vol. 173 of *Applied Mathematical Sciences*, Springer New York, New York, NY, ISBN 978-1-4419-6986-6 978-1-4419-6987-3, <https://doi.org/10.1007/978-1-4419-6987-3>, 2011.
- 510 Larocca, L. J., Twining–Ward, M., Axford, Y., Schweinsberg, A. D., Larsen, S. H., Westergaard–Nielsen, A., Luetzenburg, G., Briner, J. P., Kjeldsen, K. K., and Bjørk, A. A.: Greenland-wide accelerated retreat of peripheral glaciers in the twenty-first century, *Nature Climate Change*, pp. 1–5, <https://doi.org/10.1038/s41558-023-01855-6>, publisher: Nature Publishing Group, 2023.
- Lohmann, J. and Ditlevsen, P. D.: Risk of tipping the overturning circulation due to increasing rates of ice melt, *Proceedings of the National Academy of Sciences*, 118, e2017989118, <https://doi.org/10.1073/pnas.2017989118>, 2021.
- 515 Lohmann, J., Dijkstra, H. A., Jochum, M., Lucarini, V., and Ditlevsen, P. D.: Multistability and intermediate tipping of the Atlantic Ocean circulation, *Science Advances*, 10, eadi4253, <https://doi.org/10.1126/sciadv.adi4253>, publisher: American Association for the Advancement of Science, 2024.
- Lucarini, V. and Bódi, T.: Edge states in the climate system: exploring global instabilities and critical transitions, *Nonlinearity*, 30, R32–R66, <https://doi.org/10.1088/1361-6544/aa6b11>, 2017.
- 520 Luthcke, S. B., Zwally, H. J., Abdalati, W., Rowlands, D. D., Ray, R. D., Nerem, R. S., Lemoine, F. G., McCarthy, J. J., and Chinn, D. S.: Recent Greenland Ice Mass Loss by Drainage System from Satellite Gravity Observations, *Science*, 314, 1286–1289, <https://doi.org/10.1126/science.1130776>, 2006.



- MacAyeal, D. R.: Binge/purge oscillations of the Laurentide Ice Sheet as a cause of the North Atlantic's Heinrich events, *Paleoceanography*, 8, 775–784, <https://doi.org/10.1029/93PA02200>, 1993.
- 525 Martin, M. A., Winkelmann, R., Haseloff, M., Albrecht, T., Bueler, E., Khroulev, C., and Levermann, A.: The Potsdam Parallel Ice Sheet Model (PISM-PIK) – Part 2: Dynamic equilibrium simulation of the Antarctic ice sheet, *The Cryosphere*, 5, 727–740, <https://doi.org/10.5194/tc-5-727-2011>, publisher: Copernicus GmbH, 2011.
- McDonald, S. W., Grebogi, C., Ott, E., and Yorke, J. A.: Fractal basin boundaries, *Physica D: Nonlinear Phenomena*, 17, 125–153, [https://doi.org/10.1016/0167-2789\(85\)90001-6](https://doi.org/10.1016/0167-2789(85)90001-6), 1985.
- 530 Mehling, O., Börner, R., and Lucarini, V.: Limits to predictability of the asymptotic state of the Atlantic Meridional Overturning Circulation in a conceptual climate model, *Physica D: Nonlinear Phenomena*, 459, 134 043, <https://doi.org/10.1016/j.physd.2023.134043>, 2024.
- Meur, E. L. and Huybrechts, P.: A comparison of different ways of dealing with isostasy: examples from modelling the Antarctic ice sheet during the last glacial cycle, *Annals of Glaciology*, 23, 309–317, <https://doi.org/10.3189/S0260305500013586>, 1996.
- Morlighem, M., Williams, C. N., Rignot, E., An, L., Arndt, J. E., Bamber, J. L., Catania, G., Chauché, N., Dowdeswell, J. A., Dorschel, B., Fenty, I., Hogan, K., Howat, I., Hubbard, A., Jakobsson, M., Jordan, T. M., Kjeldsen, K. K., Millan, R., Mayer, L., Mouginot, J., Noël, B. P. Y., O'Cofaigh, C., Palmer, S., Rysgaard, S., Seroussi, H., Siegert, M. J., Slabon, P., Straneo, F., van den Broeke, M. R., Weinrebe, W., Wood, M., and Zinglensen, K. B.: BedMachine v3: Complete Bed Topography and Ocean Bathymetry Mapping of Greenland From Multibeam Echo Sounding Combined With Mass Conservation, *Geophysical Research Letters*, 44, 11,051–11,061, <https://doi.org/10.1002/2017GL074954>, _eprint: <https://onlinelibrary.wiley.com/doi/pdf/10.1002/2017GL074954>, 2017.
- 540 Oerlemans, J.: A numerical study on cyclic behaviour of polar ice sheets, *Tellus A*, 35A, 81–87, <https://doi.org/10.1111/j.1600-0870.1983.tb00187.x>, 1983.
- Papa, B. D., Mysak, L. A., and Wang, Z.: Intermittent ice sheet discharge events in northeastern North America during the last glacial period, *Climate Dynamics*, 26, 201–216, <https://doi.org/10.1007/s00382-005-0078-4>, 2006.
- Payne, A. J.: Limit cycles in the basal thermal regime of ice sheets, *Journal of Geophysical Research: Solid Earth*, 100, 4249–4263, <https://doi.org/10.1029/94JB02778>, 1995.
- 545 Ridley, J., Gregory, J. M., Huybrechts, P., and Lowe, J.: Thresholds for irreversible decline of the Greenland ice sheet, *Climate Dynamics*, 35, 1049–1057, <https://doi.org/10.1007/s00382-009-0646-0>, 2010.
- Rignot, E. and Kanagaratnam, P.: Changes in the Velocity Structure of the Greenland Ice Sheet, *Science*, 311, 986–990, <https://doi.org/10.1126/science.1121381>, 2006.
- 550 Rignot, E., Velicogna, I., van den Broeke, M. R., Monaghan, A., and Lenaerts, J. T. M.: Acceleration of the contribution of the Greenland and Antarctic ice sheets to sea level rise, *Geophysical Research Letters*, 38, <https://doi.org/10.1029/2011GL046583>, _eprint: <https://onlinelibrary.wiley.com/doi/pdf/10.1029/2011GL046583>, 2011.
- Robel, A. A., DeGiuli, E., Schoof, C., and Tziperman, E.: Dynamics of ice stream temporal variability: Modes, scales, and hysteresis, *Journal of Geophysical Research: Earth Surface*, 118, 925–936, <https://doi.org/10.1002/jgrf.20072>, 2013.
- 555 Roberts, W. H. G., Payne, A. J., and Valdes, P. J.: The role of basal hydrology in the surging of the Laurentide Ice Sheet, *Climate of the Past*, 12, 1601–1617, <https://doi.org/10.5194/cp-12-1601-2016>, publisher: Copernicus GmbH, 2016.
- Robinson, A., Calov, R., and Ganopolski, A.: An efficient regional energy-moisture balance model for simulation of the Greenland Ice Sheet response to climate change, *The Cryosphere*, 2010.
- Robinson, A., Calov, R., and Ganopolski, A.: Multistability and critical thresholds of the Greenland ice sheet, *Nature Climate Change*, 2, 429–432, <https://doi.org/10.1038/nclimate1449>, number: 6 Publisher: Nature Publishing Group, 2012.
- 560



- Robinson, A., Alvarez-Solas, J., Montoya, M., Goelzer, H., Greve, R., and Ritz, C.: Description and validation of the ice-sheet model Yelmo (version 1.0), *Geoscientific Model Development*, 13, 2805–2823, <https://doi.org/10.5194/gmd-13-2805-2020>, 2020.
- Robinson, A., Goldberg, D., and Lipscomb, W. H.: A comparison of the stability and performance of depth-integrated ice-dynamics solvers, *The Cryosphere*, 16, 689–709, <https://doi.org/10.5194/tc-16-689-2022>, 2022.
- 565 Schannwell, C., Mikolajewicz, U., Ziemen, F., and Kapsch, M.-L.: Sensitivity of Heinrich-type ice-sheet surge characteristics to boundary forcing perturbations, *Climate of the Past*, 19, 179–198, <https://doi.org/10.5194/cp-19-179-2023>, publisher: Copernicus GmbH, 2023.
- Schoof, C.: The Effect of Cavitation on Glacier Sliding, *Proceedings: Mathematical, Physical and Engineering Sciences*, 461, 609–627, <https://www.jstor.org/stable/30046308>, publisher: The Royal Society, 2005.
- Sweet, D. and Ott, E.: Fractal Dimension of Higher-Dimensional Chaotic Repellers, *Physica D: Nonlinear Phenomena*, 139, 1–27, [https://doi.org/10.1016/S0167-2789\(99\)00222-5](https://doi.org/10.1016/S0167-2789(99)00222-5), arXiv:nlin/0003014, 2000.
- 570 Swierczek-Jereczek, J., Blasco, J., Robinson, A., Alvarez-Solas, J., and Montoya, M.: Rate-induced tipping in marine-based regions of the Antarctic ice sheet, <https://doi.org/10.21203/rs.3.rs-6701284/v1>, iSSN: 2693-5015, 2025.
- The IMBIE Team: Mass balance of the Greenland Ice Sheet from 1992 to 2018, *Nature*, 579, 233–239, <https://doi.org/10.1038/s41586-019-1855-2>, 2020.
- 575 Trusel, L. D., Das, S. B., Osman, M. B., Evans, M. J., Smith, B. E., Fettweis, X., McConnell, J. R., Noël, B. P. Y., and Van Den Broeke, M. R.: Nonlinear rise in Greenland runoff in response to post-industrial Arctic warming, *Nature*, 564, 104–108, <https://doi.org/10.1038/s41586-018-0752-4>, 2018.
- Tsai, C.-Y., Forest, C. E., and Pollard, D.: Assessing the contribution of internal climate variability to anthropogenic changes in ice sheet volume, *Geophysical Research Letters*, 44, 6261–6268, <https://doi.org/10.1002/2017GL073443>, *_eprint*: <https://onlinelibrary.wiley.com/doi/pdf/10.1002/2017GL073443>, 2017.
- 580 Uppala, S. M., Kållberg, P. W., Simmons, A. J., Andrae, U., Bechtold, V. D. C., Fiorino, M., Gibson, J. K., Haseler, J., Hernandez, A., Kelly, G. A., Li, X., Onogi, K., Saarinen, S., Sokka, N., Allan, R. P., Andersson, E., Arpe, K., Balmaseda, M. A., Beljaars, A. C. M., Berg, L. V. D., Bidlot, J., Bormann, N., Caires, S., Chevallier, F., Dethof, A., Dragosavac, M., Fisher, M., Fuentes, M., Hagemann, S., Hólm, E., Hoskins, B. J., Isaksen, I., Janssen, P. A. E. M., Jenne, R., McNally, A. P., Mahfouf, J., Morcrette, J., Rayner, N. A., Saunders, R. W., Simon, P., Sterl, A., Trenberth, K. E., Untch, A., Vasiljevic, D., Viterbo, P., and Woollen, J.: The ERA-40 re-analysis, *Quarterly Journal of the Royal Meteorological Society*, 131, 2961–3012, <https://doi.org/10.1256/qj.04.176>, 2005.
- 585 Van Den Broeke, M., Bamber, J., Ettema, J., Rignot, E., Schrama, E., Van De Berg, W. J., Van Meijgaard, E., Velicogna, I., and Wouters, B.: Partitioning Recent Greenland Mass Loss, *Science*, 326, 984–986, <https://doi.org/10.1126/science.1178176>, 2009.
- Van Pelt, W. J. and Oerlemans, J.: Numerical simulations of cyclic behaviour in the Parallel Ice Sheet Model (PISM), *Journal of Glaciology*, 58, 347–360, <https://doi.org/10.3189/2012JoG11J217>, 2012.
- 590 Verjans, V., Robel, A. A., Ultee, L., Seroussi, H., Thompson, A. F., Ackerman, L., Choi, Y., and Krebs-Kanzow, U.: The Greenland Ice Sheet Large Ensemble (GrISLENS): Simulating the future of Greenland under climate variability, *EGUsphere*, pp. 1–47, <https://doi.org/10.5194/egusphere-2024-4067>, publisher: Copernicus GmbH, 2025.
- Wake, L. M., Lecavalier, B. S., and Bevis, M.: Glacial Isostatic Adjustment (GIA) in Greenland: a Review, *Current Climate Change Reports*, 2, 101–111, <https://doi.org/10.1007/s40641-016-0040-z>, 2016.
- 595 Zeitz, M., Haacker, J. M., Donges, J. F., Albrecht, T., and Winkelmann, R.: Dynamic regimes of the Greenland Ice Sheet emerging from interacting melt–elevation and glacial isostatic adjustment feedbacks, *Earth System Dynamics*, 13, 1077–1096, <https://doi.org/10.5194/esd-13-1077-2022>, publisher: Copernicus GmbH, 2022.



- 600 Ziemen, F. A., Kapsch, M.-L., Klockmann, M., and Mikolajewicz, U.: Heinrich events show two-stage climate response in transient glacial simulations, *Climate of the Past*, 15, 153–168, <https://doi.org/10.5194/cp-15-153-2019>, publisher: Copernicus GmbH, 2019.
- Zoet, L. K. and Iverson, N. R.: A slip law for glaciers on deformable beds, *Science*, 368, 76–78, <https://doi.org/10.1126/science.aaz1183>, publisher: American Association for the Advancement of Science (AAAS), 2020.